Taylor & Francis
Taylor & Francis Group

SHORT COMMUNICATION

OPEN ACCESS   Check for updates

Analogues of 2′-hydroxychalcone with modified C4-substituents as the inhibitors against human acetylcholinesterase

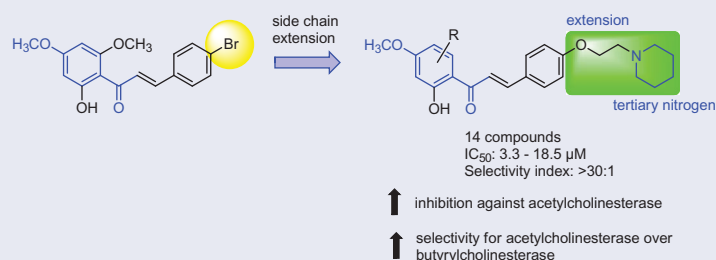Sri Devi Sukumaran[a], Shah Bakhtiar Nasir[b], Jia Ti Tee[b], Michael J. C. Buckle[a] (iD), Rozana Othman[a], Noorsaadah Abd. Rahman[b] (iD), Vannajan Sanghiran Lee[b], Syed Nasir Abbas Bukhari[c] and Chin Fei Chee[d] (iD)

aFaculty of Medicine, Department of Pharmacy, University of Malaya, Kuala Lumpur, Malaysia; bFaculty of Science, Department of Chemistry, University of Malaya, Kuala Lumpur, Malaysia; cCollege of Pharmacy, Jouf University, Al-Jouf, Kingdom of Saudi Arabia; dNanotechnology and Catalysis Research Centre, University of Malaya, Kuala Lumpur, Malaysia

ABSTRACT

A series of C4-substituted tertiary nitrogen-bearing 2′-hydroxychalcones were designed and synthesised based on a previous mixed type acetylcholinesterase inhibitor. Majority of the 2′-hydroxychalcone analogues displayed a better inhibition against acetylcholinesterase (AChE) than butyrylcholinesterase (BuChE). Among them, compound **4c** was identified as the most potent AChE inhibitor (IC$_{50}$: 3.3 μM) and showed the highest selectivity for AChE over BuChE (ratio >30:1). Molecular docking studies suggested that compound **4c** interacts with both the peripheral anionic site (PAS) and catalytic anionic site (CAS) regions of AChE. ADMET analysis confirmed the therapeutic potential of compound **4c** based on its blood–brain barrier penetrating. Overall, the results suggest that this 2′-hydroxychalcone deserves further investigation into the therapeutic lead for Alzheimer's disease (AD).

GRAPHICAL ABSTRACT

14 compounds
IC$_{50}$: 3.3 - 18.5 μM
Selectivity index: >30:1

↑ inhibition against acetylcholinesterase

↑ selectivity for acetylcholinesterase over butyrylcholinesterase

Introduction

Alzheimer's disease (AD) is the most typical form of dementia among older people which affects a person's ability to carry out daily activities. About 47 million people live with dementia worldwide and this figure is anticipated to rise to more than 131 million by 2050[1]. It has been reported that loss of cholinergic transmission is one of the major causes of AD. Therefore, small molecule cholinesterase inhibitors that enhance cholinergic transmission can be used as a remedy for AD. One such example is donepezil hydrochloride (E2020, Aricept®), which is currently used in the palliative treatment for mild to moderate AD. Analysis of the crystal structure of donepezil in complex with human AChE suggested that the benzyl, piperidine and indanone rings of donepezil are important pharmacophores for binding to the active site[2]. Subsequently, a great deal of effort has been directed towards identifying potent AChE inhibitors based on the donepezil structure, involving structure-based design and new scaffolds[3–13].

In our previous study, we have identified several 2′-hydroxychalcones that inhibited human AChE in the micromolar range and showed some selectivity for BuChE[14]. Kinetic studies indicated that these compounds were mixed-type inhibitors. Hence, the present study was undertaken to design and synthesise more potent 2′-hydroxychalcone derivatives. The synthesised derivatives were evaluated for their in vitro AChE and BuChE inhibitory activities. The Absorption, Distribution, Metabolism, Excretion and Toxicity (ADMET) parameters of these compounds were calculated. In addition, molecular modelling studies were carried out on the active compounds to gain further insight of the protein-ligand interactions.

Materials and methods

General

The chemicals and solvents used for synthesis were of analytical grade and were purchased from Sigma-Aldrich or Merck. Analytical thin-layer chromatography (TLC) was carried out on Merck precoated aluminium silica gel sheets (Kieselgel 60 F$_{254}$). Column chromatography was performed with silica gel 60

(230–400 mesh) from Merck. UV/fluorescence was measured using Infinite® M200 PRO multimode reader (Tecan Group Ltd., Männedorf, Switzerland). Melting points were taken on a Stuart melting point apparatus SMP30 (Staffordshire, UK) which has been certified for accuracy of ± 0.5 at 50 °C, ± 1.0 at 100 °C, ± 2.5 at 360 °C by the manufacturer. NMR spectra were obtained using Jeol ECA 400 (400 MHz) (Jeol Ltd., Akishima, Tokyo, Japan) or Bruker Avance III HD (600 MHz) (Bruker Biospin Corp., Billerica, MA). HRMS (ESI) analyses were performed using Agilent 1200 Series or Agilent 6530 Q-TOF (ESI) spectrometer with Agilent Zorbax C-18 column (Agilent Technologies, Santa Clara, CA). Human recombinant AChE and equine BChE were purchased from Sigma-Aldrich (St. Louis, MO).

Synthesis of 2′-hydroxychalcone derivatives

The syntheses of designed compounds **4a–h** and **8a–f** are described in the supplemental data. Their purity was checked by HPLC, ^{1}H and ^{13}C-NMR spectroscopy and mass spectrometry. The ADMET parameters of the synthesised compounds were determined using Discovery Studio v3.1 (Accelrys Inc., San Diego, CA) and SwissADME[15].

(E)-N,N-diethyl-2-(4-(3-(2-hydroxy-4-methoxyphenyl)-3-oxoprop-1-en-1yl)phenyl)acetamide (4a)

Yellow needle; yield 53%; mp 119.9–121.0 °C. ^{1}H NMR (400 MHz, CDCl$_3$): δ 13.38 (1H, s, OH), 7.78 (1H, d, $J = 15.6$ Hz, H$_\beta$), 7.75 (1H, d, $J = 8.0$ Hz), 7.52 (2H, d, $J = 8.0$ Hz), 7.48 (1H, d, $J = 15.6$ Hz, H$_\alpha$), 7.25 (2H, d, $J = 8.0$ Hz), 6.40 (1H, dd, $J = 8.0, 2.6$ Hz), 6.39 (1H, d, $J = 2.6$ Hz), 3.78 (3H, s, OCH$_3$), 3.66 (2H, s, –CH$_2$CO), 3.32 (2H, q, $J = 6.8$ Hz, –NCH$_2$–), 3.24 (2H, q, $J = 7.0$ Hz, –NCH$_2$–), 1.06 (6H, m, –CH$_3$); ^{13}C NMR (100 MHz, CDCl$_3$): δ 191.84 (C=O), 169.57 (C=O), 166.69, 166.23, 144.07, 138.44, 133.34, 131.26, 129.49, 128.81, 120.03, 114.11, 107.72, 101.10, 55.59 (OCH$_3$), 42.43 (–NCH$_2$–), 40.60 (–CH$_2$CO), 40.32 (–NCH$_2$–), 14.28 (–CH$_3$), 12.93 (–CH$_3$). HRMS calc. for [C$_{22}$H$_{25}$NNaO$_4$]$^+$ = [M + Na]$^+$ = 390.1681, found = 390.1689.

(E)-N,N-diethyl-2-(4-(3-(2-hydroxy-4,5-dimethoxyphenyl)-3-oxo-prop-1-en-1-yl)phenyl)acetamide (4b)

Yellow needles, yield 49%; mp 115.1–120 °C. ^{1}H NMR (400 MHz, CDCl$_3$): δ 13.31 (1H, s, OH), 7.80 (1H, d, $J = 15.3$ Hz, H$_\beta$), 7.54 (2H, d, $J = 8.0$ Hz), 7.42 (1H, d, $J = 15.5$ Hz, H$_\alpha$), 7.26 (2H, d, $J = 8.0$ Hz), 7.18 (1H, s), 6.43 (1H, s), 3.86, 3.84 (3H each, s, OCH$_3$), 3.68 (2H, s, –CH$_2$CO), 3.33 (2H, m, –NCH$_2$–), 3.27 (2H, m, –NCH$_2$–), 1.07 (6H, m, –CH$_3$); ^{13}C NMR (100 MHz, CDCl$_3$): δ 191.49 (C=O), 169.73 (C=O), 161.80, 157.14, 144.16, 141.99, 138.33, 133.43, 129.51, 128.84, 120.20, 112.02, 111.10, 100.85, 56.99 (OCH$_3$), 56.21 (OCH$_3$), 42.49 (–NCH$_2$–), 40.45 (–CH$_2$CO),*40.45 (–NCH$_2$–),*14.26 (–CH$_3$), 12.93 (–CH$_3$). *Resonance signal overlapped. HRMS calc. for [C$_{23}$H$_{27}$NNaO$_5$]$^+$ = [M + Na]$^+$ = 420.1787, found = 420.1798.

(E)-N,N-diethyl-2-(4-(3-(2-hydroxy-4,6-dimethoxyphenyl)-3-oxo-prop-1-en-1-yl)phenyl)acetamide (4c)

Yellow needles; Yield 40%; mp 115.5–117.2 °C. ^{1}H NMR (400 MHz, CDCl$_3$): δ 14.23 (1H, s, OH), 7.79 (1H, d, $J = 15.6$ Hz, H$_\beta$), 7.67 (1H, d, $J = 15.6$ Hz, H$_\alpha$), 7.47 (2H, d, $J = 8.3$ Hz), 7.22 (2H, d, $J = 8.3$ Hz), 6.01 (1H, d, $J = 2.0$ Hz), 5.87 (1H, d, $J = 2.0$ Hz), 3.83, 3.75 (3H each, s, OCH$_3$), 3.35 (2H, s, –CH$_2$CO), 3.31 (2H, q, $J = 7.0$ Hz, –NCH$_2$–), 3.24 (2H, q, $J = 7.0$ Hz, –NCH$_2$–), 1.05 (6H, m, –CH$_3$); ^{13}C NMR (100 MHz, CDCl$_3$): δ 192.61 (C=O), 169.71 (C=O), 168.37, 166.24,

162.53, 141.99, 137.73, 134.13, 129.35, 128.61, 127.30, 106.36, 93.84, 91.26, 55.85 (OCH$_3$), 55.56 (OCH$_3$), 42.43 (–NCH$_2$–), 40.58 (–CH$_2$CO), 40.32 (–NCH$_2$–), 14.27 (–CH$_3$), 12.93 (–CH$_3$). HRMS calc. for [C$_{23}$H$_{27}$NNaO$_5$]$^+$ = [M + Na]$^+$ = 420.1787, found = 420.1788

(E)-1-(2-hydroxy-4-methoxyphenyl)-3-(4-(2-oxo-2-(pyrrolidin-1-yl)ethyl)phenyl)prop-2-en-1-one (4d)

Yellow needles; yield 45%; mp 139.2–141.7 °C. ^{1}H NMR (400 MHz, CDCl$_3$): δ 13.37 (1H, s, OH), 7.77 (1H, d, $J = 16.0$ Hz, H$_\beta$), 7.74 (1H, d, $J = 9.0$ Hz), 7.51 (2H, d, $J = 8.0$ Hz), 7.47 (1H, d, $J = 16.0$ Hz, H$_\alpha$), 7.26 (2H, d, $J = 8.0$ Hz), 6.40 (1H, dd, $J = 8.0, 2.4$ Hz), 6.38 (1H, d, $J = 2.4$ Hz), 3.77 (3H, s, OCH$_3$), 3.62 (2H, s, –CH$_2$CO), 3.42 (2H, m, –NCH$_2$–), 3.37 (2H, m, –NCH$_2$–), 1.86 (2H, m, –CH$_2$–), 1.77 (2H, m, –CH$_2$–); ^{13}C NMR (100 MHz, CDCl$_3$): δ 191.83 (C=O), 168.57 (C=O), 166.68, 166.23, 144.07, 137.86, 133.37, 131.26, 129.76, 128.78, 120.03, 114.11, 107.71, 101.10, 55.59 (OCH$_3$), 46.95 (–NCH$_2$–), 46.05 (–NCH$_2$–), 42.02 (–CH$_2$CO), 26.13 (–CH$_2$–), 24.35 (–CH$_2$–). HRMS calc. for [C$_{22}$H$_{23}$NNaO$_4$]$^+$ = [M + Na]$^+$ = 388.1525, found = 388.1526.

(E)-1-(2-hydroxy-4,5-dimethoxyphenyl)-3-(4-(2-oxo-2-(pyrrolidin-1-yl)ethyl)phenyl)prop-2-en-1-one (4e)

Yellow needles; yield 39%; mp 149.0–150.7 °C. ^{1}H NMR (400 MHz, CDCl$_3$): δ 13.31 (1H, s, OH), 7.81 (1H, d, $J = 15.4$ Hz, H$_\beta$), 7.54 (2H, d, $J = 8.0$ Hz), 7.41 (1H, d, $J = 15.5$ Hz, H$_\alpha$), 7.29 (2H, d, $J = 8.0$ Hz), 7.18 (1H, s), 6.44 (1H, s), 3.87, 3.85 (3H each, s, OCH$_3$), 3.63 (2H, s, –CH$_2$CO), 3.41 (4H, m, –NCH$_2$–), 1.86 (2H, m, –CH$_2$–), 1.81 (2H, m, –CH$_2$–); ^{13}C NMR (100 MHz, CDCl$_3$): δ 191.49 (C=O), 169.02 (C=O), 161.80, 157.13, 144.17, 141.99, 137.77, 133.47, 129.80, 128.81, 120.22, 112.02, 111.09, 100.84, 56.99 (OCH$_3$), 56.21 (OCH$_3$), 46.94 (–NCH$_2$–), 46.29 (–NCH$_2$–), 41.94 (–CH$_2$CO), 26.11 (–CH$_2$–), 24.43 (–CH$_2$–). HRMS calc. for [C$_{23}$H$_{24}$NO$_5$]$^-$ = [M − H]$^-$ 394.1654, found = 394.1678.

(E)-2-(4-(3-(2-hydroxyphenyl)-3-oxoprop-1-en-1-yl)phenyl)acetic acid (4f)

Yellow needles; yield 61%; mp 194.1–194.6 °C. ^{1}H NMR (400 MHz, DMSO-d$_6$): δ 12.53 (1H, s, OH), 8.24 (1H, m), 8.01 (1H, d, $J = 15.5$ Hz, H$_\beta$), 7.84 (2H, d, $J = 8.0$ Hz), 7.82 (1H, d, $J = 15.5$ Hz, H$_\alpha$), 7.54 (1H, m), 7.35 (2H, d, $J = 8.0$ Hz), 7.00 (1H, dd, $J = 7.8, 2.4$ Hz), 6.98 (1H, d, $J = 2.4$ Hz), 3.63 (2H, s, –CH$_2$CO); ^{13}C NMR (100 MHz, DMSO-d$_6$): δ 194.09 (C=O), 172.75 (C=O), 162.33, 145.09, 138.71, 136.77, 133.35, 131.29, 130.54, 129.56, 121.84, 121.22, 119.64, 118.20, 41.03 (–CH$_2$CO). HRMS calc. for [C$_{17}$H$_{15}$O$_4$]$^+$ = [M + H]$^+$ = 283.0970, found = 283.0979.

(E)-2-(4-(3-(2-hydroxy-5-methoxyphenyl)-3-oxoprop-1-en-1-yl)phenyl)acetic acid (4g)

Orange powders; yield 44%; mp 91.7–93.6 °C. ^{1}H NMR (400 MHz, CDCl$_3$): δ 12.36 (1H, s, OH), 7.88 (1H, d, $J = 15.6$ Hz, H$_\beta$), 7.60 (2H, d, $J = 8.0$ Hz), 7.55 (1H, d, $J = 15.6$ Hz, H$_\alpha$), 7.34 (2H, d, $J = 8.0$ Hz), 7.33 (1H, d, $J = 2.5$ Hz), 7.13 (1H, dd, $J = 7.8, 2.5$ Hz), 6.96 (1H, d, $J = 8.0$ Hz), 3.83 (3H, s, OCH$_3$), 3.76 (2H, s, –CH$_2$CO); ^{13}C NMR (100 MHz, CDCl$_3$): δ 193.46 (C=O), 170.65 (C=O), 158.01, 151.80, 145.32, 138.34, 133.30, 129.75, 129.08, 123.99, 120.02, 119.72, 119.44, 113.00, 56.25 (OCH$_3$), 40.84 (–CH$_2$CO). HRMS calc. for [C$_{18}$H$_{17}$O$_5$]$^+$ = [M + H]$^+$ = 313.1071, found = 313.1036.

(E)-2-(4-(3-(2-hydroxy-4,6-dimethoxyphenyl)-3-oxoprop-1-en-1-yl)phenyl)acetic acid (4h)

Yellow powders; yield 58%; mp 139.2–141.2 °C. ^{1}H NMR (400 MHz, CDCl$_3$): δ 14.21 (1H, s, OH), 7.79 (1H, d, $J = 15.6$ Hz, H$_\beta$), 7.68 (1H, d, $J = 15.6$ Hz, H$_\alpha$), 7.48 (2H, d, $J = 8.0$ Hz), 7.21 (2H, d, $J = 8.0$ Hz), 6.02 (1H, d, $J = 2.2$ Hz), 5.88 (1H, d, $J = 2.2$ Hz), 3.83, 3.76 (3H each, s, OCH$_3$), 3.70 (2H, s, –CH$_2$CO); ^{13}C NMR (100 MHz, CDCl$_3$): δ 192.60 (C=O), 169.01 (C=O), 168.38, 166.26, 162.53, 141.93, 137.53, 134.15, 129.25, 128.68, 127.35, 106.37, 93.85, 91.29, 55.88 (OCH$_3$), 55.58 (OCH$_3$), 40.79 (–C̲H$_2$CO). HRMS calc. for [C$_{19}$H$_{19}$O$_6$]$^+$ = [M + H]$^+$ = 343.1182, found = 343.1194.

(E)-1-(2-hydroxy-4-methoxyphenyl)-3-(4-(2-(piperidin-1-yl)ethoxy)phenyl)prop-2-en-1-one (8a)

Yellow solid; yield 67%; mp 166.7–169.7 °C. ^{1}H NMR (600 MHz, CDCl$_3$ (90%) and MeOH-d_4 (10%)): δ 13.45 (1H, brs, OH), 7.76 (1H, d, $J = 15.9$ Hz, H$_\beta$), 7.74 (1H, d, $J = 8.0$ Hz), 7.52 (2H, d, $J = 8.0$ Hz), 7.37 (1H, d, $J = 15.4$ Hz, H$_\alpha$), 6.87 (1H, d, $J = 8.0$ Hz), 6.40 (1H, d, $J = 7.8$ Hz), 6.39 (1H, s), 4.24 (2H, brt, –CH$_2$–), 3.78 (3H, s, OCH$_3$), 2.94 (2H, brt, –CH$_2$–), 2.69 (4H, brs, –NCH$_2$–), 1.70 (4H, brs, –CH$_2$–), 1.46 (2H, brs,–CH$_2$–); ^{13}C NMR (150 MHz, CDCl$_3$): δ 191.97 (C=O), 166.09, 165.97, 160.01, 143.98, 131.30, 130.35, 128.11, 118.27, 114.95, 114.02, 107.53, 100.96, 63.97 (–OCH$_2$–), 56.70 (–CH$_2$N–), 55.45 (–NCH$_2$–), 54.37 (OCH$_3$), 23.96 (–CH$_2$–), 22.55 (–CH$_2$–). HRMS calc. for [C$_{23}$H$_{28}$NO$_4$]$^+$ = [M + H]$^+$ = 382.2018, found = 382.2036.

(E)-1-(2-hydroxy-4-methoxyphenyl)-3-(4-(2-(pyrrolidin-1-yl)ethoxy)phenyl)prop-2-en-1-one (8b)

Yellow needles; yield 72%; mp 189.9–192.1 °C. ^{1}H NMR (600 MHz, CDCl$_3$): δ 13.44 (1H, brs, OH), 7.77 (1H, d, $J = 15.0$ Hz, H$_\beta$), 7.74 (1H, d, $J = 9.0$ Hz), 7.53 (2H, d, $J = 8.5$ Hz), 7.38 (1H, d, $J = 15.4$ Hz, H$_\alpha$), 6.89 (2H, d, $J = 8.5$ Hz), 6.42 (1H, dd, $J = 9.0, 2.0$ Hz), 6.39 (1H, s), 4.32 (2H, t, $J = 5.0$ Hz, –CH$_2$–), 3.78 (3H, s, OCH$_3$), 3.20 (2H, t, $J = 5.0$ Hz, –CH$_2$–), 3.02 (4H, brs, –NCH$_2$–), 1.95 (4H, brs, –CH$_2$–); ^{13}C NMR (150 MHz, CDCl$_3$): δ 191.88 (C=O), 166.14, 166.10, 159.90, 143.91, 131.26, 130.41, 128.33, 118.46, 115.06, 114.12, 107.62, 101.06, 64.79 (–OCH$_2$–), 55.58 (–CH$_2$N–), 54.64 (OCH$_3$), 54.25 (–NCH$_2$–), 23.26 (–CH$_2$–). HRMS calc. for [C$_{22}$H$_{26}$NO$_4$]$^+$ = [M + H]$^+$ = 368.1862, found = 368.1885.

(E)-1-(2-hydroxy-4,5-dimethoxyphenyl)-3-(4-(2-(piperidin-1-yl)ethoxy)phenyl)prop-2-en-1-one (8c)

Dark red needles; yield 61%; mp 145.0–146.2 °C. ^{1}H NMR (600 MHz, CDCl$_3$): δ 13.37 (1H, s, OH), 7.78 (1H, d, $J = 15.4$ Hz, H$_\beta$), 7.54 (2H, d, $J = 8.6$ Hz), 7.32 (1H, d, $J = 15.5$ Hz, H$_\alpha$), 7.20 (1H, s), 6.88 (2H, d, $J = 8.6$ Hz), 6.43 (1H, s), 4.38 (2H, t, $J = 3.6$ Hz, –CH$_2$–), 3.86, 3.85 (3H each, s, OCH$_3$), 3.20 (2H, t, $J = 3.0$ Hz, –CH$_2$–), 2.99 (4H, brs, –NCH$_2$–), 1.85 (4H, m, –CH$_2$–), 1.54 (2H, brs, –CH$_2$–); ^{13}C NMR (150 MHz, CDCl$_3$): δ 191.45 (C=O), 161.73, 159.75, 157.04, 143.96, 141.76, 130.44, 128.43, 118.53, 115.08, 112.04, 111.17, 100.84, 63.83 (–OCH$_2$–), 57.05 (–CH$_2$N–), 56.66 (–NCH$_2$–), 56.19 (OCH$_3$), 54.44 (OCH$_3$), 23.61 (–CH$_2$–), 22.51 (–CH$_2$–). HRMS calc. for [C$_{24}$H$_{30}$NO$_5$]$^+$ = [M + H]$^+$ = 412.2124, found = 412.2130.

(E)-1-(2-hydroxy-4,5-dimethoxyphenyl)-3-(4-(2-(pyrrolidin-1-yl)ethoxy)phenyl)prop-2-en-1-one (8d)

Orange solid; yield 58%; mp 167.0–169.0 °C. ^{1}H NMR (600 MHz, CDCl$_3$): δ 13.35 (1H, s, OH), 7.78 (1H, d, $J = 15.4$ Hz, H$_\beta$), 7.55 (2H, d, $J = 8.7$ Hz), 7.34 (1H, d, $J = 15.4$ Hz, H$_\alpha$), 7.19 (1H, s), 6.90 (2H, d,

$J = 8.7$ Hz), 6.44 (1H, s), 4.49 (2H, t, $J = 4.5$ Hz, –CH$_2$–), 3.87, 3.86 (3H each, s, OCH$_3$), 3.42 (2H, t, $J = 4.6$ Hz, –CH$_2$–), 3.33 (4H, brs, –NCH$_2$–), 2.09 (4H, brs, –CH$_2$–); ^{13}C NMR (150 MHz, CDCl$_3$): δ 191.43 (C=O), 161.75, 159.37, 157.04, 143.84, 141.96, 130.49, 128.75, 118.74, 115.09, 112.03, 111.09, 100.85, 63.91 (–OCH$_2$–), 57.03 (–CH$_2$N–), 56.21 (–NCH$_2$–), 54.55 (OCH$_3$), 54.05 (OCH$_3$), 23.27 (–CH$_2$–). HRMS calc. for [C$_{23}$H$_{28}$NO$_5$]$^+$ = [M + H]$^+$ = 398.1967, found = 398.1968.

(E)-1-(2-hydroxy-4,6-dimethoxyphenyl)-3-(4-(2-(piperidin-1-yl)ethoxy)phenyl)prop-2-en-1-one (8e)

Yellow needles; yield 69%; mp 164.3–166.7 °C. ^{1}H NMR (600 MHz, CDCl$_3$): δ 14.30 (1H, s, OH), 7.73 (1H, d, $J = 15.6$ Hz, H$_\beta$), 7.68 (1H, d, $J = 15.6$ Hz, H$_\alpha$), 7.47 (2H, d, $J = 8.4$ Hz), 6.85 (2H, d, $J = 8.4$ Hz), 6.03 (1H, s), 5.89 (1H, s), 4.28 (2H, t, $J = 5.0$ Hz, –CH$_2$–), 3.85, 3.76 (3H each, s, OCH$_3$), 2.98 (2H, t, $J = 5.0$ Hz, –CH$_2$–), 2.75 (4H, brs, –NCH$_2$–), 1.74 (4H, m, –CH$_2$–), 1.48 (2H, brs, –CH$_2$–); ^{13}C NMR (150 MHz, CDCl$_3$): δ 192.55 (C=O), 168.36, 166.09, 162.47, 159.72, 142.13, 130.13, 128.92, 125.56, 114.98, 106.35, 93.83, 91.25, 64.61 (–OCH$_2$–), 57.07 (–CH$_2$N–), 55.87 (OCH$_3$), 55.58 (–NCH$_2$–), 54.60 (OCH$_3$), 24.41 (–CH$_2$–), 23.09 (–CH$_2$–). HRMS calc. for [C$_{24}$H$_{30}$NO$_5$]$^+$ = [M + H]$^+$ = 412.2124, found = 412.2131.

(E)-1-(2-hydroxy-4,6-dimethoxyphenyl)-3-(4-(2-(pyrrolidin-1-yl)ethoxy)phenyl)prop-2-en-1-one (8f)

Yellow solid; yield 70%; mp 157.0–159.0 °C. ^{1}H NMR (600 MHz, CDCl$_3$): δ 14.27 (1H, s, OH), 7.73 (1H, d, $J = 15.5$ Hz, H$_\beta$), 7.67 (1H, d, $J = 15.5$ Hz, H$_\alpha$), 7.48 (2H, d, $J = 8.6$ Hz), 6.89 (2H, d, $J = 8.6$ Hz), 6.03 (1H, d, $J = 2.3$ Hz), 5.89 (1H, d, $J = 2.3$ Hz), 4.50 (2H, t, $J = 4.4$ Hz, –CH$_2$–), 3.85, 3.77 (3H each, s, OCH$_3$), 3.45 (2H, t, $J = 4.4$ Hz, –CH$_2$–), 3.35 (4H, brs, –NCH$_2$–), 2.10 (4H, brs, –CH$_2$–); ^{13}C NMR (150 MHz, CDCl$_3$): δ 192.52 (C=O), 168.37, 166.17, 162.50, 158.75, 141.71, 130.18, 129.68, 126.10, 115.04, 106.35, 93.85, 91.28, 63.55 (–OCH$_2$–), 55.89 (–CH$_2$N–), 55.59 (OCH$_3$), 54.54 (OCH$_3$), 54.01 (–NCH$_2$–), 23.26 (–CH$_2$–). HRMS calc. for [C$_{23}$H$_{28}$NO$_5$]$^+$ = [M + H]$^+$ = 398.1967, found = 398.1973.

Enzyme inhibition studies

To determine the inhibitory activity of the target compounds towards cholinesterases, the AChE and BuChE inhibition assays were performed in 96 well plates by the method of Ellman with slight modifications[16]. First, sodium phosphate buffer (110 μL; pH 8.0) was added into each well followed by 20 μL of each test compound, 50 μL of 5,5'-dithiobis-(2-nitrobenzoic acid) (DTNB) (0.126 mM) and 20 μL of AChE or BuChE (0.15 units per mL). Then, the mixture was incubated for 20 min at 37 °C. Subsequently, the reaction was initiated by addition of 50 μL (0.120 mM) of the substrate, acetylthiocholine (ATC) iodide or butyrylthiocholine (BTC) iodide (depending on the enzyme). The hydrolysis of ATC or BTC was monitored with an Infinite® M200 PRO multimode reader (Tecan Group Ltd., Männedorf, Switzerland) by measuring the absorbance of the yellow 5-thio-2-nitrobenzoate anion at 412 nm, every 30 s for 25 min. Donepezil, propidium iodide and tacrine were used as standard inhibitors. Each assay was performed in triplicate. The percentage of inhibition was calculated using the following expression:

$$(E–S)/E \times 100$$

where E is the activity of the enzyme without test compound and S is the activity of the enzyme with the test compound. IC$_{50}$

values were obtained from concentration-inhibition experiments by nonlinear regression analysis using PRISM® v5.0 (GraphPad Inc., San Diego, CA).

Molecular modelling studies

Three-dimensional structural models of the test compounds were built using Chem Bio-3D v13 (CambridgeSoft, Cambridge, MA) and saved in MOL2 format. The compounds were then prepared in a protonated form, where appropriate for physiological pH, and minimised using Hyperchem Pro v6.0 (geometry optimisation – MM$^+$) to give the lowest energy conformation. The X-ray crystal structure of human AChE in complex with donepezil was retrieved from the Protein Data Bank (PDB ID: 4EY7)[2]. Ligand and water molecules were removed using Discovery Studio v3.1. Hydrogen atoms were added and double coordinates were corrected using Hyperchem Pro v6.0 (Hypercube Inc., Gainesville, FL). Hydrogen atoms were again added, non-polar hydrogen atoms were merged, and missing atoms were repaired using AutoDock Tools v4[17]. Gasteiger charges were added and AutoDock v4.0 type atoms were assigned to the protein. Then, test compounds were randomly docked into the protein structure with AutoDock v4.0 using a hybrid Lamarckian Genetic Algorithm[18], with an initial population size of 150 and a maximum number of 2,500,000 energy evaluations. The grid box was set to cover the entire protein with a spacing of 0.375 Å. The root mean square deviation (RMSD) tolerance was set to 2.0 Å for the clustering of docked results and the docked pose of each ligand was selected on the basis of free energy of binding and cluster analysis.

Ligand–protein interactions were analysed using Discovery Studio v3.1 and PoseView[19].

Results and discussion

Design strategy

Docking of the corresponding 2′-hydroxy-4′,6′-dimethoxy-4-bromochalcone (Figure 1) described in our previous work to the crystal structure of the human AChE (PDB ID: 4EY7) reveals room for a possible side-chain extension from the C4 position to engage extra binding interactions[14]. The docking structure suggests that the indole ring of Trp86 at the bottom of the active site gorge is a perspective binding site by π-cation interaction. Thus, we focussed on a well-established chain extension strategy which involves the incorporation of a tertiary nitrogen functional group linked into the C4 position of 2′-hydroxychalcone via a short alkyl chain[20]. We designed and synthesised a set of 14 target derivatives by varying substituent at the C4 position to increase the potency (Table 2, compounds **4a–h** and **8a–f**).

Chemistry

The syntheses of target derivatives are outlined in Scheme 1. The amide coupling between 4-(hydroxymethyl)phenylacetic acid **1** and the corresponding amine was conducted under the standard carbodiimide chemistry afforded compound **2**, which was further oxidised to benzaldehyde **3** with periodinane. The 2′-hydroxychalcone derivatives **4a–h** were obtained from the Claisen-Schmidt condensation of different substituted 2′-hydroxyacetophenones

Scheme 1. Syntheses of tertiary nitrogen-bearing 2′-hydroxychalcones. Reaction conditions: (a) EDC, HOBt, R$_1$NH, CH$_2$Cl$_2$, 18 h, 28 °C (b) Dess-Martin periodinane, CH$_2$Cl$_2$, 18 h, 28 °C (c) 2′-hydroxyacetophenone, 50% aqueous NaOH, MeOH, 24 h, 28 °C (d) MOM-Cl, Et$_3$N, CH$_2$Cl$_2$, 4 h, 28 °C (e) 1 M HCl, MeOH, 2 h, 60 °C (f) 1-(2-chloroethyl)piperidine·HCl or 1-(2-chloroethyl)pyrrolidine·HCl, Cs$_2$CO$_3$, NaI, acetone, 24 h, 60 °C.

Figure 1. Design strategy for 2′-hydroxychalcones with modified C4-substituents.

Table 1. ADMET parameters for 2′-hydroxychalcones **4a–h** and **8a–f**.

Compound	MW	HBD	HBA	Log P	PSA(Å^2)	AS	GIA	BBB
4a	367.44	1	4	3.59	67.70	Moderate	High	Yes
4b	397.46	1	5	3.57	76.63	Moderate	High	Yes
4c	397.46	1	5	3.57	76.63	Moderate	High	Yes
4d	365.42	1	4	3.35	67.70	Moderate	High	Yes
4e	395.45	1	5	3.34	76.63	Moderate	High	Yes
4f	282.29	2	4	3.12	76.23	Soluble	High	Yes
4g	312.32	2	5	3.11	85.16	Soluble	High	No
4h	342.34	2	6	3.09	94.10	Soluble	High	No
8a	381.46	1	5	4.48	59.33	Moderate	High	Yes
8b	367.44	1	5	4.03	59.33	Moderate	High	Yes
8c	411.49	1	6	4.47	68.26	Moderate	High	Yes
8d	397.46	1	6	4.01	68.26	Moderate	High	Yes
8e	411.49	1	6	4.47	68.26	Moderate	High	Yes
8f	397.46	1	6	4.01	68.26	Moderate	High	Yes
Donepezil	379.49	0	4	4.57	38.51	Moderate	High	Yes
Propidium	414.59	2	2	3.40	58.43	Moderate	High	No
Tacrine	198.26	1	2	2.79	37.80	Moderate	High	Yes

MW: molecular weight; HBD: number of hydrogen bond donors; HBA: number of hydrogen bond acceptors; log P: logarithm of octanol–water partition coefficient; PSA: polar surface area. AS: aqueous solubility; GIA: gastrointestinal absorption; BBB: blood–brain barrier.

and benzaldehyde **3** in the presence of NaOH in methanol[14]. Compound **7** was synthesised in a similar fashion by using different substituted 2′-hydroxyacetophenones and methoxymethyl ether (MOM) protected benzaldehyde **6**. Finally, compounds **8a–f** were generated from compound **7** with 1-(2-chloroethyl)piperidine hydrochloride or 1-(2-chloroethyl)pyrrolidine hydrochloride in the presence of Cs_2CO_3 and NaI[21]. All target compounds **4a–h** and **8a–f** were purified by silica gel chromatography. Their structures were confirmed by using nuclear magnetic resonance spectroscopy (^{1}H NMR, ^{13}C NMR) and high-resolution mass spectrometry (HRMS). Representative spectroscopic spectra are provided in the supplemental data.

ADMET parameters

The predicted ADMET parameters of designed compounds **4a–h** and **8a–f** are summarised in Table 1. According to the ADMET analysis, all the compounds follow Lipinski's rule by causing no violation[22–24]. Compounds **4g** and **4h** are predicted by the SwissADME to be unable to cross the blood–brain barrier[15]. Despite the designed compounds are moderately soluble in water, they have a high degree of gastrointestinal absorption. This may be due to the presence of tertiary nitrogen atom in these compounds that allow the formation of salt, resulting in improved solubility and gastrointestinal adsorption.

Cholinesterase inhibitory activity

The designed 2′-hydroxychalcone derivatives were evaluated for their *in vitro* inhibitory activities against human recombinant AChE according to Ellman's colorimetric assay method[16]. The results are summarised in Table 2. Most of the tested compounds showed promising AChE inhibitory activity when screened at 10 μM. Based on the structure–activity relationship analysis, it is clear that AChE inhibitory activity was closely related to the C4-substituent. Generally, the tertiary amine substituted compounds possessed better AChE inhibitory activity than that of tertiary amide substituted compounds. The results of **8a**, **8b**, and **8d–f** demonstrated that compounds with piperidine or pyrrolidine substituted at C4 position were comparably potent as that of donepezil and tacrine against AChE. When examining the efficacy of compounds **4a–e**, the presence of 6′-methoxy substituent in the A ring favour the AChE

Table 2. Substituent patterns and human acetylcholinesterase inhibitory activity of 2′-hydroxychalcones **4a–h** and **8a–f**.

Compound	Structure	Human AChE (% Inhibition at 10 μM)[a]
4a		67.2
4b		58.5
4c		87.5
4d		30.8
4e		58.9
4f		10.7
4g		27.0
4h		15.6
8a		79.9
8b		83.0
8c		52.5
8d		80.6
8e		83.6
8f		81.4
Donepezil[b]		92.0
Propidium[c]		52.0
Tacrine[d]		89.0

[a]Values are expressed as mean of triplicate; [b]standard PAS and CAS-binding AChE inhibitor; [c]standard PAS-binding AChE inhibitor; [d]standard CAS-binding AChE inhibitor.

activity. Compounds **4f–h** which lack of a tertiary nitrogen substituent in B ring were inactive, indicating that the carboxylic group is not favoured for interaction. Besides, the length of the C4 side chain also played a significant role in the AChE inhibitory activity. Tertiary amine-bearing derivatives **8a–f** which contain a side chain of 2 carbon atoms, displayed a better inhibition than those derivatives without side chain described in our previous work[14].

Subsequently, IC_{50} experiments were carried out for compounds **4c**, **8a**, **8b**, and **8d–f** against human AChE and equine BuChE. The latter is considered a good model for human BuChE due to its high sequence similarity to the human form (90%

Table 3. Human AChE and equine BuChE inhibitory activities of the most active tertiary nitrogen containing 2′-hydroxychalcones.

Compound	Human AChE $IC_{50}/\mu M^a$	Equine BuChE $IC_{50}/\mu M^a$	Selectivity index[b]
4c	3.3 ± 1.3	>100	>30
8a	4.2 ± 1.3	>100	>24
8b	12.8 ± 4.8	65.6 ± 14.8	5.1
8d	15.9 ± 1.8	89.9 ± 12.0	5.7
8e	4.6 ± 0.9	18.3 ± 8.0	4.0
8f	18.5 ± 3.8	31.3 ± 8.2	1.7
Donepezil[c]	0.09 ± 0.01	1.9 ± 0.2	21
Propidium[d]	11 ± 3	20.8 ± 2.1	1.9
Tacrine[e]	0.19 ± 0.04	0.011 ± 0.001	0.06

[a]Values are expressed as mean of triplicate; [b]Selectivity index = IC_{50} (BuChE)/IC_{50} (AChE); [c]Standard PAS and CAS-binding AChE inhibitor; [d]Standard PAS-binding AChE inhibitor; [e]Standard CAS-binding AChE inhibitor.

sequence identity)[25]. The IC_{50} values are included in Table 3. Generally, these compounds showed higher activity towards AChE with IC_{50} values in the range of 3–19 μM. Among the target derivatives, compound **4c** was the most active towards AChE with IC_{50} = 3.3 μM. Moreover, compound **4c** exhibited the highest selectivity for AChE over BuChE (SI >30). High AChE selectivity over BuChE (SI >24) was also observed for compound **8a**, which possesses a piperidinyl ethyl ether substituted at the C4 position. Studies have shown that high AChE selectivity over BuChE may reduce the associated side effects of AD treatment[26]. Hence, compounds with high AChE selectivity over BuChE may be clinically useful. As can be seen in Table 3, the designed compounds generally showed lower BuChE inhibitory activity as compared to that of AChE. Compound **8e** was the most active towards BuChE with IC_{50} = 18.3 μM. In comparison, compound **8a** which lack of a 6′-methoxy substituent in the A ring was inactive, indicating that the 6′-methoxy group is important for interaction.

Molecular docking

The most active compounds **4c**, **8a**, and **8e** were docked into an AChE model obtained from the X-ray crystal structure of human AChE in complex with donepezil (PDB ID: 4EY7)[2] in order to study the protein–ligand binding interactions.
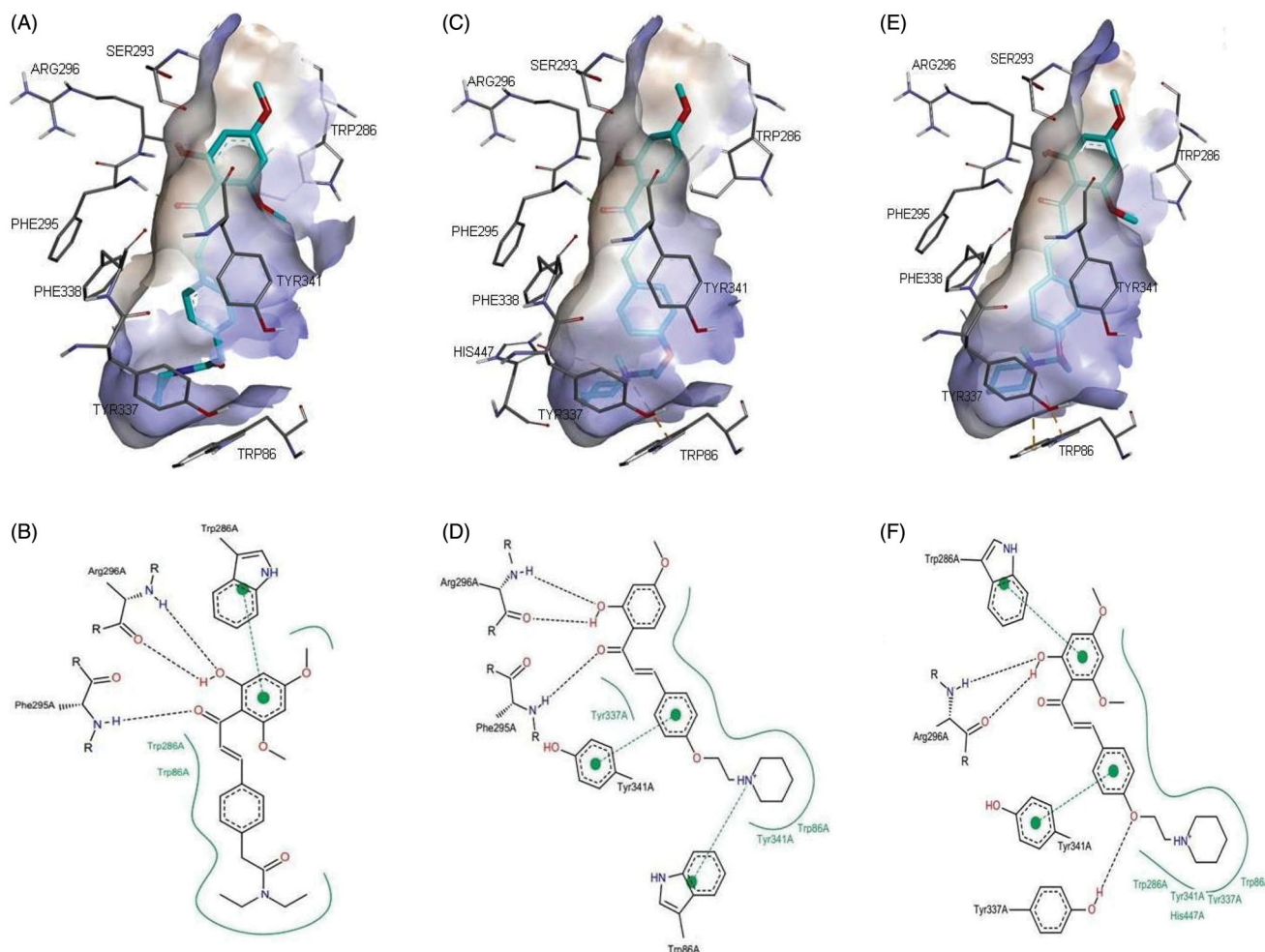

Figure 2. Representations of compounds **4c** (A, B), **8a** (C, D), and **8e** (E, F) in complex with human AChE (PDB ID: 4EY7). (A, C, and E) 3D representations of the binding pose. The hydrophobic surfaces of the interacting residues are shown in blue relief. Hydrogen bonds and π–cation interactions are depicted with green and orange dotted lines, respectively; (B, D, and F) Schematic representations of the binding interactions. Hydrogen bonds and π–π stacking interactions are depicted with black and green dotted lines, respectively. The green curve represents other non-polar interactions.

All docked compounds were found to exhibit binding poses similar to those of donepezil occupying both the peripheral anionic site (PAS) and catalytic anionic site (CAS) of the AChE (Figure 2). It was observed that the aromatic ring A of compounds **4c** and **8e** formed $\pi-\pi$ stacking interactions with the PAS residue, Trp286, whereas aromatic ring B of compound **8a** formed $\pi-\pi$ stacking interactions with Tyr341 (at the entrance to the gorge leading to that CAS). In the case of compounds **4c** and **8a**, the carbonyl oxygen atom and the *ortho*-hydroxyl group on the A ring were observed to form hydrogen bonds with backbone atoms from acyl pocket residues, Phe295 and Arg296, respectively. This may be one of the reasons to account for the greater activity of these two compounds, as compound **8e** only interacted with Arg296. The positively-charged nitrogen atom of the piperidine ring in compound **8a** formed $\pi-$cation interaction with CAS site aromatic residue, Trp86. This interaction is particularly important as several studies have reported its implication for biological recognition of human AChE[27,28]. In the case of compound **8e**, an extra hydrogen bonding interaction was formed between the ether oxygen atom and residue Tyr337. Taken together, these interactions have contributed to the enhanced potency of 2′-hydroxychalcone with modified C4-substituents. The docking findings are in agreement with the experimental results and provide reasons for improved cholinesterase inhibitory activity of the designed derivatives.

Conclusions

In conclusion, novel 2′-hydroxychalcone derivatives with modified C4-substituents were designed, synthesised and evaluated as inhibitors of human AChE. Compounds with methoxy substituents on the A ring and piperidinyl ethyl ether substituent on B ring were generally found to be more potent. Molecular docking studies have suggested that these compounds interact with both the PAS and CAS regions of AChE. The most active 2′-hydroxychalcones showed high AChE selectivity over BuChE, suggesting that these compounds may be suitable to be developed into clinically useful drug candidates.

Authors' contributions

S.D.S: biological evaluation, chemical synthesis, molecular modelling, and manuscript drafting. T.J.T, S.B.N.: chemical synthesis. C.F.C., M.J.C.B.: project design, data analysis, manuscript preparation and revision. S.N.A.B.: interpretation of data and manuscript revision. R.O., N.A.R, and V. S. L: Project conception, design and co-ordination. All authors have read and approved the final version of the manuscript.

Disclosure statement

No potential conflict of interest was reported by the author(s).

ORCID

Michael J. C. Buckle http://orcid.org/0000-0003-2438-2376

Noorsaadah Abd. Rahman http://orcid.org/0000-0001-5847-8961
Chin Fei Chee http://orcid.org/0000-0002-5650-9119

Data availability statement

The raw data supporting the conclusions of this manuscript will be made available by the authors, without undue reservation, to any qualified researcher.

References

1. Alzheimer's Association. 2018 Alzheimer's disease facts and figures. Alzheimers Dement 2018;14:367–425.
2. Cheung J, Rudolph MJ, Burshteyn F, et al. Structures of human acetylcholinesterase in complex with pharmacologically important ligands. J Med Chem 2012;55:10282–6.
3. van Greunen DG, Cordier W, Nell M, et al. Targeting Alzheimer's disease by investigating previously unexplored chemical space surrounding the cholinesterase inhibitor donepezil. Eur J Med Chem 2017;127:671–90.
4. Peauger L, Azzouz R, Gembus V, et al. Donepezil-based central acetylcholinesterase inhibitors by means of a "bio-oxidizable" prodrug strategy: design, synthesis, and in vitro biological evaluation. J Med Chem 2017;60:5909–26.
5. Lan JS, Zhang T, Liu Y, et al. Design, synthesis and biological activity of novel donepezil derivatives bearing n-benzyl pyridinium moiety as potent and dual binding site acetylcholinesterase inhibitors. Eur J Med Chem 2017;133:184–96.
6. Xie SS, Lan JS, Wang XB, et al. Design, synthesis and biological evaluation of novel donepezil-coumarin hybrids as multi-target agents for the treatment of alzheimer's disease. Bioorg Med Chem 2016;24:1528–39.
7. Wang ZM, Cai P, Liu QH, et al. Rational modification of donepezil as multifunctional acetylcholinesterase inhibitors for the treatment of alzheimer's disease. Eur J Med Chem 2016;123:282–97.
8. Li F, Wang ZM, Wu JJ, et al. Synthesis and pharmacological evaluation of donepezil-based agents as new cholinesterase/monoamine oxidase inhibitors for the potential application against alzheimer's disease. J Enzym Inhib Med Chem 2016;31:41–53.
9. Huang CS, Tu WT, Luo M, Shi JC. Molecular docking and design of novel heterodimers of donepezil and huperzine fragments as acetylcholinesterase inhibitors. Chin J Struct Chem 2016;35:839–48.
10. Costanzo P, Cariati L, Desiderio D, et al. Design, synthesis, and evaluation of donepezil-like compounds as ache and bace-1 inhibitors. ACS Med Chem Lett 2016;7:470–5.
11. Desiderio D, Lamberti A, Roberta S, et al. Donepezil analogs as acetylcholinesterase inhibitors. FEBS J 2014;281:557.
12. Hu YQ, Zhang J, Chandrashankra O, et al. Design, synthesis and evaluation of novel heterodimers of donepezil and huperzine fragments as acetylcholinesterase inhibitors. Bioorg Med Chem 2013;21:676–83.
13. Ismail MM, Kamel MM, Mohamed LW, Faggal SI. Synthesis of new indole derivatives structurally related to donepezil and their biological evaluation as acetylcholinesterase inhibitors. Molecules 2012;17:4811–23.
14. Sukumaran SD, Chee CF, Viswanathan G, et al. Synthesis, biological evaluation and molecular modelling of 2-hydroxychalcones as acetylcholinesterase inhibitors. Molecules 2016; 21:955.

15. Daina A, Michielin O, Zoete V. Swissadme: a free web tool to evaluate pharmacokinetics, drug-likeness and medicinal chemistry friendliness of small molecules. Sci Rep 2017;7: 42717.

16. Ellman GL, Courtney KD, Andres V, Jr., Feather-Stone RM. A new and rapid colorimetric determination of acetylcholinesterase activity. Biochem Pharmacol 1961;7:88–95.

17. Morris GM, Huey R, Lindstrom W, et al. AutoDock4 and AutoDockTools4: automated docking with selective receptor flexibility. J Comput Chem 2009;30:2785–91.

18. Morris GM, Goodsell DS, Halliday RS, et al. Automated docking using a Lamarckian genetic algorithm and empirical binding free energy function. J Comput Chem 1998;19:1639–62.

19. Stierand K, Maass PC, Rarey M. Molecular complexes at a glance: automated generation of two-dimensional complex diagrams. Bioinform 2006;22:1710–16.

20. Leong SW, Abas F, Lam KW, et al. 2-benzoyl-6-benzylidene-cyclohexanone analogs as potent dual inhibitors of acetyl-cholinesterase and butyrylcholinesterase. Bioorg Med Chem 2016;24:3742–51.

21. Gao XH, Zhou C, Liu HR, et al. Tertiary amine derivatives of chlorochalcone as acetylcholinesterase (ache) and buthyl-cholinesterase (buche) inhibitors: the influence of chlorine, alkyl amine side chain and α,β-unsaturated ketone group. J Enzyme Inhib Med Chem 2017;32:146–52.

22. Lipinski CA, Lombardo F, Dominy BW, Feeney PJ. Experimental and computational approaches to estimate solubility and permeability in drug discovery and development settings. Adv Drug Deliv Rev 1997;23:3–25.

23. Kelder J, Grootenhuis PDJ, Bayada DM, et al. Polar molecular surface as a dominating determinant for oral absorption and brain penetration of drugs. Pharm Res 1999;16:1514–19.

24. Van de Waterbeemd H, Camenish G, Folkers G, et al. Estimation of blood-brain barrier crossing of drugs using molecular size and shape, and H-bonding descriptors. J Drug Target 1998;6:151–65.

25. Sawatzky E, Wehle S, Kling B, et al. Discovery of highly selective and nanomolar carbamate-based butyrylcholinesterase inhibitors by rational investigation into their inhibition mode. J Med Chem 2016;59:2067–82.

26. Li Y, Qiang X, Luo L, et al. Aurone mannich base derivatives as promising multifunctional agents with acetylcholinesterase inhibition, anti-β-amyloid aggragation and neuroprotective properties for the treatment of Alzheimer's disease. Eur J Med Chem 2017;126:762–75.

27. Ranjan A, Chauhan A, Jindal T. In-silico and in-vitro evaluation of human acetylcholinesterase inhibition by organophosphates. Environ Toxicol Pharmacol 2018;57:131–40.

28. Nachon F, Carletti E, Ronco C, et al. Crystal structures of human cholinesterases in complex with huprine w and tacrine: elements of specificity for anti-Alzheimer's drugs targeting acetyl-and butyryl-cholinesterase. Biochem J 2013; 453:393–9.